Development of an optimized trend kriging model using regression analysis and selection process for optimal subset of basis functions

Hakjin Lee[1], Duck-Joo Lee[1,*] and Hyungil Kwon[2]

[1]*Korea Advanced Institute of Science and Technology (KAIST), Daejeon, 305-701, Republic of Korea*

[2]*Hyundai Motor Group, Hwaseong-si, Gyeonggi-do, 445-706, Republic of Korea*

Abstract

Surrogate modeling, or metamodeling, is an efficient way of alleviating the high computational cost and complexity for iterative function evaluation in design optimization. Accuracy is significantly important because optimization algorithms rely heavily on the function response calculated by surrogate model and the optimum solution is directly affected by the quality of surrogate model. In this study, an optimized trend kriging model is proposed to improve the accuracy of the existing kriging models. Within the framework of the proposed model, regression analysis is carried out to approximate the unknown trend of the true function and to determine the order of the universal kriging model, which has a fixed form with a mean structure dependent on the order of model. In addition, the selection of an optimal basis function is conducted to separate the useful basis function terms from the full set of the basis function. The optimal subset of the basis function is selected with the global optimization algorithm; which can accurately represent the trend of true response surface. The mean structure of proposed model has been optimized to maximize the accuracy of kriging model depending on the trend of true function. Two- and three-dimensional analytic functions and a practical engineering problem are chosen to validate the proposed model. The results showed that the OTKG model yield the most accurate responses regardless of the number of initial sample points, and can conversed into well-trained model with few additional sample points.

Keywords: Kriging surrogate model, Trend function, Regression analysis, Coefficient of determination, Genetic Algorithms, Design optimization.

[*] Corresponding author.
E-mail address : djlee@kaist.ac.kr

1. Introduction

Industry and academia have continuously been attempting to solve engineering design problems with complex geometry and a highly unsteady flow because computing performance has been continuously growing. To find the optimal solution of engineering system, the objective and constraint functions as a function of the design variables have to be iteratively evaluated. However, high-fidelity analysis of the complex configuration, such as an airplane including the pylon and the intake or the unsteady simulation of rotary systems (e.g., helicopter rotors, wind turbines, and open rotor systems), still requires a computing time of several hours or days to obtain the converged solutions. It is nearly impossible for high-fidelity analysis to be directly applied to the design optimization process because of high computational costs and resources. The surrogate model, which is often called a metamodeling is an efficient way to alleviate this computational burden. It represents a true response surface using a simple mathematical function with evaluated function values of sample points. Then, the iterative and expensive function evaluation can be substituted for modeled response surface instead of actual simulation. Therefore, the accuracy of the surrogate model is significant because the optimization results are significantly affected by the quality of the surrogate model. However, constructing high-fidelity surrogate model for complex problems with numerous variables are challenging because large number of variables has much influence on the efficiency of the optimization process. P. Hao et al. suggested a bi-step surrogate-based optimization framework with adaptive sampling to build high-fidelity surrogate modes with less computational cost for complex engineering designs. [1]

Several surrogate models have been developed, such as polynomial response surfaces, Artificial Neural Networks (ANN) [2, 3], Genetic Programming (GP) [4], Support Vector Regression (SVR) [5], the Radial Basis Function (RBF) [6], Moving Least Squares (MLS), and the Kriging model [7]. The kriging model is one of the most attractive models because it has a good capability of dealing with nonlinear response. Although the true function is explicitly unknown, the kriging model can provide statistical error information that is modeled using a Gaussian process as well as the predicted function response at an untried point. Therefore, it is widely used in various research fields, including spatial analysis, mathematical geology, and engineering.

The fundamental formulation of the kriging model is consisted of the two parts: the drift function and the deviation function. The former represents the global trend of the kriging model, while the latter is a localized variation between the true and the drift functions. The accuracy of the kriging model relies greatly on how to formulate them. Many studies have been conducted to improve the accuracy of the kriging model. H.S. Chung and

J.J. Alonso used secondary information, such as the values of the gradient, in addition to primary function values at sample points for constructing a covariance matrix of the deviation terms [8]. Z.H. Han et al. suggested a new Cokriging model that utilized both the function values at sample points obtained by the variable fidelity analysis and gradient values computed by the adjoint method to generate the kriging model [9, 10]. Their results show that the accuracy of the kriging model can be enhanced by using the gradient information and the function values computed by variable fidelity analysis. They have focused on the modification of deviation terms to improve the quality of the kriging model. In contrast, V.R. Joseph et al. proposed the blind kriging model that uses the optimally selected basis functions to model the trend function. The optimal subset of basis functions can be selected by the Bayesian forward selection process [11]. However, the Bayesian forward selection process could easily get stuck in the local optimum solution rather than finding the global optimum. This converging problem was overcome in dynamic kriging model which was suggested by L. Zhao et al. In dynamic kriging model, the optimization problem of selecting basis functions from the candidates of basis functions was solved by using genetic algorithm which is one of the most popular global optimization algorithm. The kriging process variance was used as the objective function of the optimization problem for finding the optimal subset of basis function. It was found that the quality of the kriging model can be enhanced by excluding unnecessary polynomial terms in the full set of basis function [12]. However, H. Liang and M. Zhu pointed out that the kriging process variance cannot be set to be the objective function of the optimization problem for searching optimal basis functions and genetic algorithm cannot converge to the global optimum. It is analytically proved [13]. A revised dynamic kriging model has been proposed to design the trend function using cross-validation method, and the cross-validation root mean-square error and cross-validation error correlation coefficients were used to be the objective function in the optimization problem of designing the trend function [14]. To find the optimal subset of basis function in the optimization problem, the highest-order of trend function needs to be determined first. In dynamic and revised dynamic kriging model, it is determined to satisfy a constraint associated with the number of samples and the total number of possible candidates of basis functions. However, this constraint depends strongly on the number of sample points and does not consider the trend of the true response. H.I. Kwon and S.I. Choi has developed the R^2 indicator based on regression analysis. The coefficient of determination, denoted R^2 indicates that how well the regression model can approximate the trend of sample points. The unknown trend of the true response could be approximately predicted, and the well-matched order of the universal kriging (UKG) model can be determined depending on the coefficients of determination. It is called the

trended kriging (TKG) model because its mean structure is constructed to fit the trend of the true response more accurately by considering the trend of the true function. The results showed that the TKG can improve the accuracy of the model by adjusting its drift function to the identified trend of the true function [15]. However, the form of the drift function in the mean structure is fixed as a *p-th* order polynomial function. Although the order of the drift function is properly determined from the regression analysis, the unnecessary terms in the fixed form of the drift function could deteriorate the quality of the kriging model.

In this study, an optimized trend kriging (OTKG) model is suggested to improve the accuracy of the TKG model by excluding the unnecessary terms from full set of basis function in mean structure. Therefore, we adopted the global optimization algorithm to separate the useful terms from the fixed form of the basis function of the TKG. In order to validate the OTKG model and compare its accuracy with the ordinary kriging (OKG) model and the UKG models, two- and three-dimensional analytic functions were applied. The validation results verified that the proposed OTKG model can be applied to any trend of response and provide a more accurate response surface than existing kriging models. The proposed OTKG model was also applied to a practical engineering problem. The numerical example shows that the OTKG model can more accurately represent the true response, despite a lack in the number of sample points.

The outline of this paper is as follows. The methods for the optimized OTKG model, including the basic background of the kriging model, trend identification and optimal basis selection process, are introduced in the following section. The detailed validation procedure and the results of using two- and three dimensional analytic functions are described in section 3. Section 4 explains a practical engineering problem and shows the results of model comparison, depending on the dimension of the problem, and the accuracy of the proposed model and the existing model are compared. Our conclusions are discussed in Section 5.

2. Background and methods

2.1 Kriging model

The kriging model was initially suggested to find locations for a borehole by D.G. Krige [7] and mathematically formulated by G. Matheron [16]. It is an interpolation-based surrogate model and perfectly passes through all sample points which are extracted by the Design of Experiment (DoE) approach. The function values of selected sample points must be evaluated by numerical simulation or experimentation. In the kriging model, the deterministic

form of the true function is assumed to be the stochastic form of the function. As mentioned above, the kriging model is modeled as the sum of the drift function and the deviation function, as shown by Eq. (1). The first term on the right-hand side of Eq. (1) is the mean structure of the model that globally presents and emulates a mean trend of the true response, while the second term is a deviation between the true and drift functions.

$$\mathbf{y} = \mathbf{F}\boldsymbol{\beta} + \mathbf{Z} \tag{1}$$

The drift function in the kriging model can be formulated using the *p-th* order polynomial function which is called as *p-th* order universal kriging (UKG) model. Its drift function can be written as shown by Eqs. (2)–(4), where $\mathbf{y}$ is the vector of the response values at the sample points, $\mathbf{x}$ is the vector of the sample points ($\mathbf{x} = [\mathbf{x}_1, \mathbf{x}_2, \cdots, \mathbf{x}_m]^T$ with $\mathbf{x}_i \in \boldsymbol{R}^n$), n is the number of design variables (the dimension of the design space), and m is the number of sample points. In this study, the Latin Hypercube Sampling (LHS) method is used to randomly select the sample points in the design space. It is known that the LHS method is well-fitted to the kriging model [17]. $\mathbf{F}$ is the $m \times k$ model matrix that is composed of the *p-th* order polynomial form of the basis function, where k is the number of elements in the full basis function, $\mathbf{f}(\mathbf{x})$. $\boldsymbol{\beta}$ is the vector of the regression coefficients for the polynomial function that is determined with the Generalized Least Square (GLS) method [18].

$$\mathbf{y} = \left[y(\mathbf{x}_1), y(\mathbf{x}_2), \ldots, y(\mathbf{x}_m) \right]^T \tag{2}$$

$$\mathbf{F} = \left[f_k(\mathbf{x}_i) \right] = \begin{bmatrix} f_1(\mathbf{x}_1) & f_2(\mathbf{x}_1) & \cdots & f_k(\mathbf{x}_1) \\ f_1(\mathbf{x}_2) & f_2(\mathbf{x}_2) & \cdots & f_k(\mathbf{x}_2) \\ \vdots & \vdots & \ddots & \\ f_1(\mathbf{x}_m) & f_2(\mathbf{x}_m) & \cdots & f_k(\mathbf{x}_m) \end{bmatrix} \tag{3}$$

$$\boldsymbol{\beta} = [\beta_1, \beta_2, \ldots, \beta_k]^T \tag{4}$$

In the kriging model, the deviation function, Eq. (5), is stochastically modeled to have zero mean and σ^2 variance by assuming a normal distributed Gaussian process. In order to consider the relationship among sample points, the covariance model must be defined as in Eq. (6), where $\mathbf{R}$ is the $m \times m$ correlation matrix, and σ^2 is the process variance. The correlation matrix has a symmetric and positive definite form and consists of the spatial correlation function, R, that is used to express the influence exerted by two sample points on each other. In this research, the correlation function is expressed with the Gaussian form [19], as shown in Eq. (8), where $x_{i,l}$ is the lth component of the vector of $\mathbf{x}_i$. If the distance between the sample points is further increased, the correlation is exponentially decreased.

$$\mathbf{Z} = \left[Z(\mathbf{x_1}), Z(\mathbf{x_2}), \ldots, Z(\mathbf{x}_m)\right]^T \tag{5}$$

$$Cov\left(Z(\mathbf{x}_i), Z(\mathbf{x}_j)\right) = \sigma^2\, \mathbf{R}\left[R(\boldsymbol{\theta}, \mathbf{x}_i, \mathbf{x}_j)\right] \tag{6}$$

$$\mathbf{R}\left[R(\boldsymbol{\theta}, \mathbf{x}_i, \mathbf{x}_j)\right] = \begin{bmatrix} R(\boldsymbol{\theta}, \mathbf{x}_1, \mathbf{x}_1) & R(\boldsymbol{\theta}, \mathbf{x}_1, \mathbf{x}_2) & \cdots & R(\boldsymbol{\theta}, \mathbf{x}_1, \mathbf{x}_m) \\ R(\boldsymbol{\theta}, \mathbf{x}_2, \mathbf{x}_1) & R(\boldsymbol{\theta}, \mathbf{x}_2, \mathbf{x}_2) & \cdots & R(\boldsymbol{\theta}, \mathbf{x}_2, \mathbf{x}_m) \\ \vdots & \vdots & \ddots & \\ R(\boldsymbol{\theta}, \mathbf{x}_m, \mathbf{x}_1) & R(\boldsymbol{\theta}, \mathbf{x}_m, \mathbf{x}_2) & \cdots & R(\boldsymbol{\theta}, \mathbf{x}_m, \mathbf{x}_m) \end{bmatrix} \tag{7}$$

$$R(\boldsymbol{\theta}, \mathbf{x}_i, \mathbf{x}_j) = \prod_{l=1}^{n} \exp\left(-\theta_l (x_{i,l} - x_{j,l})^2\right) \tag{8}$$

In Eq. (8), $\boldsymbol{\theta}$ is defined as the correlation parameter, which determines the radius of influence. Therefore, the smoothness of the kriging response depends on its value. It should be optimally estimated to build the most suitable model. The optimal value of the correlation parameter can be obtained with the Maximum Likelihood Estimation (MLE), which is widely utilized to statistically estimate model parameters. The likelihood function for MSE can be defined with Eq. (9), since the kriging model is assumed to have a Gaussian distribution at any point in the design space. However, the estimation of the optimal correlation parameter using the MLE function may lead to complex and tedious calculations. Therefore, the MLE function is rearranged as in Eq. (10), and optimization algorithms are applied to solve the unconstrained optimization problem and find the optimal correlation parameter [20]. In this research, the Pattern Search Algorithm is employed to accurately solve the optimization problem in Eq. (10).

$$L(\mathbf{x}_1, \ldots, \mathbf{x}_m, \boldsymbol{\theta}) = \left(\frac{1}{2\pi\sigma^2}\right)^{m/2} \left(\frac{1}{|\mathbf{R}|}\right)^{1/2} \exp\left(-\frac{1}{2\sigma^2}(\mathbf{y} - \mathbf{F}\boldsymbol{\beta})^T \mathbf{R}^{-1} (\mathbf{y} - \mathbf{F}\boldsymbol{\beta})\right) \tag{9}$$

$$\text{minimize} \quad \psi(\theta) = \frac{1}{2}[m \ln(\sigma_z^2) + \ln(|\mathbf{R}|)] \tag{10}$$

If we obtain the correlation parameter by solving the above minimization problem, the other parameters for the kriging model can be simply evaluated with Eqs. (11) and (12). After estimating these model parameters, the final form of the kriging model can be formulated with Eq. (13) at an untried point. Although the true response is unknown, the kriging model can also provide the mean squared error (MSE), which is statistically modeled using probability theory using Eq. (14).

$$\frac{\partial(\ln L)}{\partial \boldsymbol{\beta}} = 0 : \quad \hat{\boldsymbol{\beta}} = (\mathbf{F}^T \mathbf{R}^{-1} \mathbf{F})^{-1} \mathbf{F}^T \mathbf{R}^{-1} \mathbf{y_s} \tag{11}$$

$$\frac{\partial(\ln L)}{\partial \sigma^2} = 0 : \quad \hat{\sigma}^2 = \frac{1}{m}(\mathbf{y} - \mathbf{F}\hat{\boldsymbol{\beta}})^T \mathbf{R}^{-1} (\mathbf{y} - \mathbf{F}\hat{\boldsymbol{\beta}}) \tag{12}$$

$$\hat{y}(\mathbf{x}) = \mathbf{f}(\mathbf{x})^T \hat{\boldsymbol{\beta}} + \mathbf{r}(\mathbf{x})^T \mathbf{R}^{-1}(\mathbf{y} - \mathbf{F}\hat{\boldsymbol{\beta}}) \tag{13}$$

$$MSE[\hat{y}(\mathbf{x})] = \hat{\sigma}^2(1 - \mathbf{r}(\mathbf{x})^T \mathbf{R}^{-1}\mathbf{r}(\mathbf{x}) + \mathbf{u}(\mathbf{x})^T(\mathbf{F}^T\mathbf{R}^{-1}\mathbf{F})^{-1}\mathbf{u}(\mathbf{x})) \tag{14}$$

$$\text{where} \quad \mathbf{u}(\mathbf{x}) = \mathbf{F}^T\mathbf{R}^{-1}\mathbf{r}(\mathbf{x}) - \mathbf{f}(\mathbf{x})$$

2.2 Trend identification

In the UKG model, if the order of the model is determined, then the form of the mean structure will be fixed as the *p-th* order polynomial function consisting full set of the basis function. The proper mean structure that matches well with the trend of the true function would lead to a better quality model response. However, the wrong mean structure could not properly fit the global trend of the true function, resulting in decreased accuracy of the kriging model, as reported in D. Zimmerman et al. [21] and J.D. Martin and T. W. Simpson [22]. Therefore, the order of the polynomial function must be carefully determined. It would be quite helpful if we can approximately predict the trend of the true function before constructing the kriging model. The order of the UKG can be simply determined from a constraint, as shown in Eq. (15). The total number of possible candidate basis functions cannot be larger than the number of samples that was proposed by L. Zhao et al. [12] and H. Liang et al. [14]. However, this constraint depends strongly on the number of sample points and does not consider the trend of the true response. In order to identify the trend of the true response and determine the order of the UKG model, the R^2 trend indicator, based on the coefficient of determination, was suggested by H.I. Kwon and S.I. Choi [15]. They have verified that the trend of the true function can be identified from the coefficient of determination, and the order of the UKG model can be determined based on its value. The UKG model, using a drift function corresponding to the trend of the true function, more accurately represents the true response compared to the OKG and other order UKG models. This model is called the trended kriging (TKG) model. In this study, the R^2 trend indicator, which was based on the coefficient of determination, is used to identify the trend of the true data before constructing the OTKG model.

$${}_{n+p}C_p = \frac{(n+p)!}{n!\,p!} \le m - 1 \tag{15}$$

Regression analysis is a statistical process used to assess the fitness of regression models. The coefficient of determination, denoted R^2, can be evaluated through regression analysis, as shown by Eqs. (16) and (17). It is a statistical value that indicates how well the regression model presents or emulates the set of dependent variables; it ranges from 0 to 1. In Eq. (17), s is the number of sample points for regression analysis, y_i is the set of the true responses at the sample points, $\bar{y}$ is the mean value of the true responses, and $\hat{y}_i$ is the set of the predicted response

values from a linear regression model. To accurately assess the coefficient of regression, a large number of sample points for regression analysis is required. This may cause serious concerns for computing time. Therefore, the function values for the regression analysis are computed by using the preliminary response surfaces: the OKG model for linear trend identification and the 1st order derivative of the OKG model for nonlinear trend identification. The schematic procedures for trend identification are shown in Fig. 1. Through the procedure for trend identification, we can statistically predict the trend of the true response and determine the order of the UKG model. This UKG model will be used as a baseline model for the proposed OTKG model. A source for a detailed description of the R^2 trend indicator is listed in the references [15].

$$R^2 = \frac{SSR}{SST} = \frac{SSR}{SSE + SSR} \tag{16}$$

$$SST = \sum_{i=1}^{s} (y_i - \bar{y})^2 \quad SSR = \sum_{i=1}^{s} (\hat{y}_i - \bar{y})^2 \quad SSE = \sum_{i=1}^{s} (y_i - \hat{y}_i)^2 \tag{17}$$

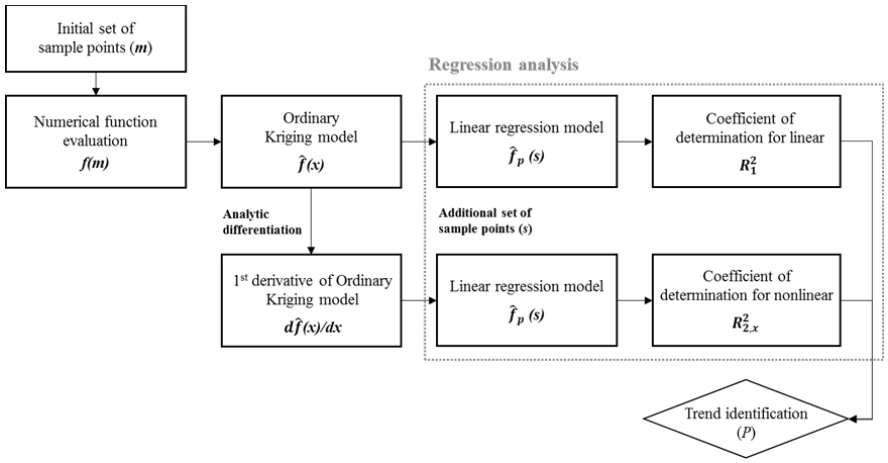

Fig. 1 Schematic procedure for the trend identification using the regression analysis.

2.3 Optimal basis function selection

In the previous section, we explained how to predict the trend of the true response through regression analysis when determining the order of the UKG model, which is utilized as the baseline for the OTKG model. The total number of terms in the full basis function is ${}_{n+p}C_p$, where n is the number of design variables and p is the order of the UKG model. For example, when n is 3 and p is 2, the number of the polynomial terms in the full basis function is 10, and $\mathbf{f} = [1, x_1, x_2, x_3, x_1^2, x_1x_2, x_1x_3, x_2^2, x_2x_3, x_3^2]$ is the full set of basis function, which is employed to build the mean structure of trend function. However, this mean structure could deteriorate the quality of the model due to

unnecessary terms in the full set of the basis function. In this section, we will describe how to select the optimal subset of the basis function from the full basis function. The optimal subset of the basis function included only terms that could lead to the improvement of accuracy by excluding unnecessary terms.

An optimization algorithm is needed to sort the optimal terms from the full basis function. For this research, we adopted the genetic algorithm (GA), which is one of the most popular Evolutionary Algorithms (EAs), inspired by the natural evolution processes of humans (including inheritance, mutation, selection, and crossover). The detailed advantages of using the GA method are described by L. Zhao et al. [12]. The GA is a particularly attractive method and widely used to solve many design optimization problems because it does not require the gradient information. It randomly searches the overall design space to find the optimal solution based only on the fitness values of candidates without the gradient information. Therefore, it is less likely to get stuck at the local minima. The binary-coded Non-Dominated Sorting Genetic Algorithm (NSGA-II), developed by K. Deb et al. [23, 24], is applied to search for the optimal subset of the basis function. In order to conduct the genetic operation, the population must be defined for every generation. A binary-coded NSGA-II generates a single string of ${}_{n+p}C_p$-bit encoding that is a binary number: 0 or 1. Each binary number in the string is directly allocated to each respective polynomial term in the full basis function of the *p-th* order UKG model. Whether the assigned polynomial term should be used is determined by the binary number, where 1 indicates that the polynomial term is selected as a candidate, and 0 indicates that the polynomial term is not selected. As a result, the population for finding the optimal basis function is defined by combining the polynomial basis function with the single string of binary numbers. The objective function must also be defined to compare the fitness value of the population and decide which population will survive from the current generation to the next generation. If the true function is explicitly known, the true root mean squared error (RMSE) value, which is the discrepancy between the true and model functions, can easily be calculated at any position in the design domain. However, the true RMSE value is not available in practical engineering design problems, since the true function is not explicitly given. As we mentioned in a previous section, although the true function is not known, the kriging model can provide the values for the model MSE, which is statistically derived from probability theory. In this study, evenly distributed grid points, denoted *e*, are employed to calculate the model MSEs, and their sum is used in the objective function of the genetic operation. The low sum of model MSEs implies that kriging model can properly represent the true response and accurately provide the predicted function values. Thus, finding the optimal subset of the basis function from the full basis function is equivalent to minimizing the

sum of the kriging model MSEs, as formulated in Eq. (18). The binary-coded NSGA-II program is adopted to solve the following unconstrained optimization problem.

$$\begin{aligned} &\textbf{minimize} \quad && I = \sum_{i=1}^{e} MSE[\,\hat{\mathrm{y}}_j(\mathbf{x}_i)] \\ &\textbf{subject to} \quad && \mathbf{f}_j(\mathbf{x}) \end{aligned} \tag{18}$$

The NSGA-II and the kriging model are interactively coupled and iteratively share key information with each other, including the current and next candidates and their fitness values. The selection process is iteratively conducted until a convergence condition is satisfied. In this study, the NSGA-II will be complete if the maximum number of iterations reaches the number of generations. The overall process for the OTKG model will be described in next section.

2.4 Framework for optimized trend kriging model

The proposed framework for constructing the OTKG model is illustrated in Fig. 2. The gray shaded parts are the most important parts of the proposed framework; they illustrate trend identification using the coefficient of determination and the selection of the optimal basis function using the optimization algorithm. The initial sample points are randomly extracted by the LHS method, and function evaluation is carried out by a numerical simulation, such as CFD. Regression analysis is conducted to identify the trend of the true function and to assess the coefficient of determination by using preliminary kriging models. The preliminary kriging models for linear and nonlinear trend identification are the OKG and the 1st order derivative of the OKG model, respectively. The former is constructed using the set of the initial sample that is evaluated by CFD, while the latter is analytically derived from the OKG model. Based on the values of the coefficients of determination, we can approximately predict whether the true response has a linear or nonlinear trend and determine the order of the UKG model that is used as a baseline for the OTKG model. After the order of the UKG model is determined, the optimization algorithm is adopted to find the optimal subset of the basis function that will maximize the kriging model accuracy and minimize its MSE. In this framework, the NSGA-II code and the UKG model are tightly coupled. They interactively and iteratively share the data with each other until the termination criterion is satisfied. If the form of the basis function is changed during the optimization process, the optimization problem in Eq. (10) must be repeatedly solved to newly estimate the correlation parameter. It is a time consuming task. However, updating the correlation parameter to adjust the

changed form of the basis function has little impact on the optimization results, as reported in L. Zhao [12]. Therefore, the correlation parameter is assumed to remain constant during the optimization process. The constant correlation parameter is set to the optimal value obtained from the baseline model, the *p-th* order UKG model.

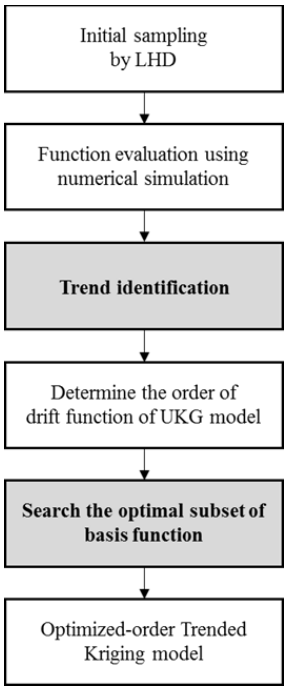

Fig. 2 Proposed framework for constructing optimized trend kriging model.

3. Validation

3.1 Analytic functions

In the previous section, the framework for constructing the OTKG model and the detailed method were described. The proposed model needs to be validated to demonstrate how it can improve accuracy compared to existing OKG, UKG, and TKG models. To compare the accuracy of kriging models, we deliberately select the well-known polynomial form of two analytic functions. Test function 1 is the two-dimensional Six-Hump Camelback function, which is a 6^{th} order polynomial function and has six local minima, two of which are the global minima. Test function 2 is the three-dimensional Rosenbrock function, which has several local minima and one global minimum inside a long, narrow, parabolic-shaped valley. They are widely used to test the performance of the optimization algorithm in design optimization problems. Detailed descriptions, including the dimension, domain, and the results of regression analysis, of test functions 1 and 2 are listed in Tables 1 and 2, and the mathematical

form of the functions are given by Eqs. (19) and (20). In Tables 1 and 2, the coefficients of determination for linear or nonlinear trend identification are the mean values for 40 consecutive trials with different sets of the sample points (because they depend significantly on the sample positions). The regression analysis results show that both test function 1 and 2 are highly nonlinear in both the x_1 and x_2 directions. Therefore, the 2nd order UKG model is selected as the baseline model for both test function 1 and 2, and the optimal subset of the basis function will be sorted from the full set of the 2nd order basis function.

$$f(x_1,x_2)=\left(4-2.1x_1^2+\frac{x_1^4}{3}\right)x_1^2+x_1x_2+\left(-4+4x_2^2\right)x_2^2 \tag{19}$$

$$f(x_1,x_2,x_3)=100(x_2-x_1^2)^2+(x_1-1)^2+100(x_3-x_2^2)^2+(x_2-1)^2 \tag{20}$$

The quality of surrogate model can be assessed by three different metrics including root mean squared error (RMSE), average error, and maximum error [25]. In order to assess the accuracy of kriging models, three metrics are evaluated and compared. It turned out that their trend are almost similar. In current research, the model and true RMSEs are chosen as comparison metrics for comparison in analytic and practical problems, respectively. The former can be simply estimated with the kriging model, as in Eq. (14), while the latter is generally not available because the true function is unknown in many practical engineering problems. In this section, since the explicit forms of the analytic function are already known, the true RMSE value computed at the given testing grid points is used to compare the accuracy of the kriging models. In Eq. (21), the RMSE is the value of the true root mean squared error, $\boldsymbol{x}_i$ is the testing point, $y(\boldsymbol{x}_i)$ is the value of the true response, and $\hat{y}(\boldsymbol{x}_i)$ is the value of the predicted response from the kriging model.

$$RMSE=\sqrt{\frac{1}{e}\sum_{i=1}^{e}\left[y(\mathbf{x}_i)-\hat{y}(\mathbf{x}_i)\right]^2} \tag{21}$$

The quality of the kriging model is directly affected by the number of samples and the specific sample profile. In order to eliminate the effect of random sampling on the accuracy of the kriging model, the model comparison was conducted over 40 trials with different sample profiles. The model comparison was also carried out with various numbers of initial samples to confirm the robustness of the proposed framework. For test functions 1 and 2, the mean true RMSE values for 40 trials, depending on the number of initial samples, are listed in Tables 3 and 4.

Table 1 Detailed description of test function 1

Parameter	Values
Dimension of function	2
Domain of function	$x_1 \in$ [-3, 3], $x_2 \in$ [-2, 2]
Coefficient of determination for linear	0.0208
Coefficient of determination for nonlinear	(0.7126, 0.7806)

Table 2 Detailed description of test function 2

Parameter	Values
Dimension of function	3
Domain of function	$x_i \in$ [-5, 10], i = 1,⋯,3
Coefficient of determination for linear	0.3926
Coefficient of determination for nonlinear	(0.8588, 0.8346, 0.2944)

3.2 Results and discussion

As previously mentioned, the model comparison was carried out over 40 trials with different sample profiles to eliminate the effect of random sampling, given the number of initial samples. The number of initial sample points has been changed from 15 to 35 for test function 1 and 20 to 40 for test function 2. The model comparison using the analytic function has been performed based on the mean true RMSE value from each surrogate model because the exact function values can be easily obtained at any point

As indicated in Tables 3-4 and Fig. 3-4, the model comparison results for both test function 1 and 2 showed that the proposed OTKG model resulted in the most accurate response compared to the OKG and other UKG models, regardless of the number of samples. It is worth noting that, the smaller the number of sample points, the better the proposed OTKG model fit the true response for all model comparison results. In other words, the OTKG model converged into a well-matured model with few additional sample points. The OKG and UKG models require more sample points to secure the level of accuracy of the OTKG model. Thus, when the number of sample points is small, the OTKG model is much more useful than other models. The results from one trial for test function 1 are illustrated in Fig. 5 and Fig. 6. For test function 1, the true (red shaded) and model (gray shaded) response surfaces can be seen in Fig. 5; the values were calculated from the true function and the kriging models, respectively. The true error contours in Fig. 6 show the disparity between the models. The black dots on the response surfaces, or contours, are the set of initial sample points. As can be observed from Fig. 5 and 6, the OTKG model has a well-matched response

surface, and the true error was significantly decreased by excluding the unnecessary terms from the full set of the basis function. However, for test function 2, we cannot plot the response surfaces and directly compare the true error because it is a three-dimensional function. Therefore, we cut the plane along the x_3 direction to plot the true error contours. The results from one trial for test function 2 are illustrated in Fig. 7. Again, we found that the OTKG model yields significantly more accurate results compared with the OKG and UKG models.

Table 3 Mean true RMSEs over 40 trials of test function 1

m	OKG	UKG1	UKG2	OTKG
15	22.9239	23.7326	17.9126	14.9871
20	21.1179	22.4075	16.6084	14.4523
25	18.1388	18.7021	14.5924	13.0610
30	13.8784	14.1842	12.0220	11.1248
35	11.2699	11.5928	9.5175	8.8300

Table 4 Mean true RMSEs over 40 trials of test function 2

m	OKG	UKG1	UKG2	OTKG
20	27.7882	23.5901	15.4513	12.0981
25	23.3393	19.7873	14.3585	11.7156
30	18.6651	15.9767	12.9087	10.8123
35	12.7481	12.7775	10.9925	9.5217
40	9.8197	11.1388	8.6812	7.7929

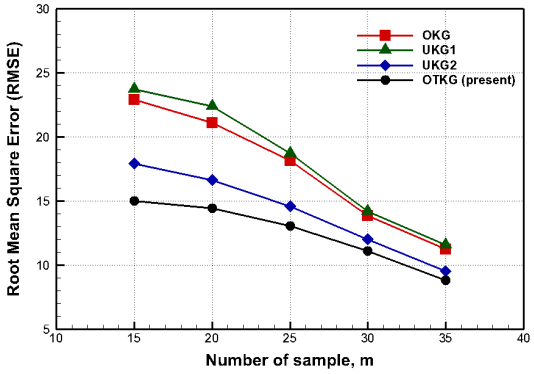

Fig. 3 Comparison of mean true RMSEs for test function 1.

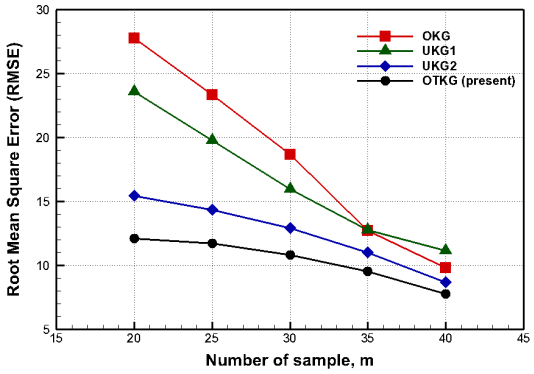

Fig. 4 Comparison of mean true RMSEs for test function 2.

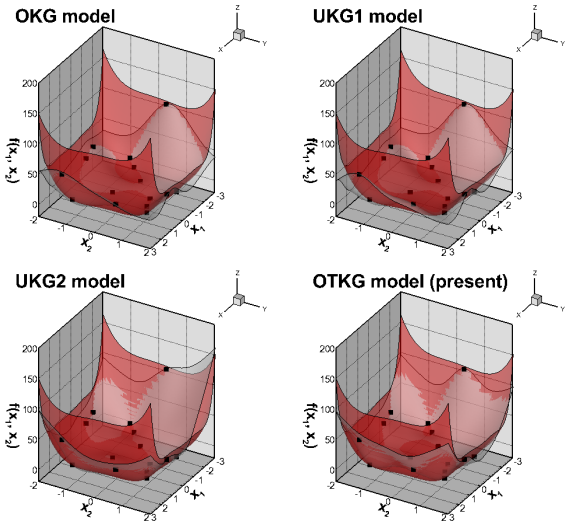

Fig. 5 Comparison of true and model responses of test function 1.

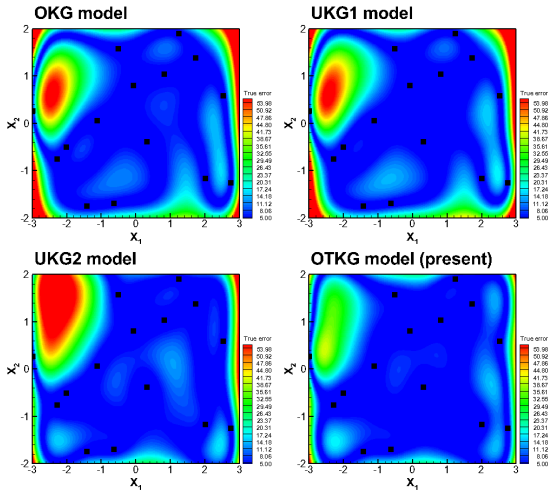

Fig. 6 Comparison of true error contours of test function 1.

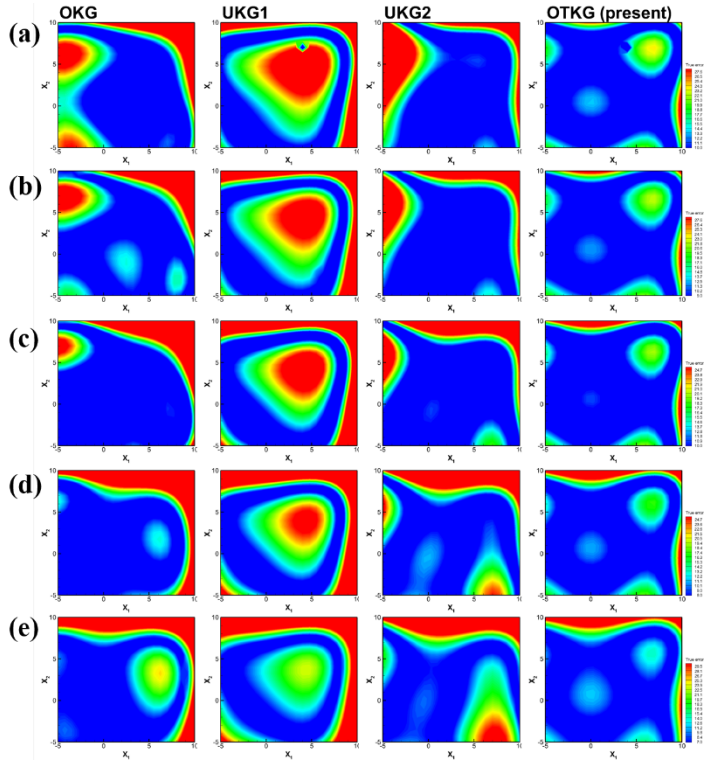

Fig. 7 Comparison of true error contours along x_3 direction for test function 2: x_3/D = (a) 1.0, (b) 0.75, (c) 0.50, (d) 0.25, and (e) 0.0

4. Application

In the previous section, two analytic functions with different dimensions were used to validate the accuracy of the OTKG model compared to the OKG and UKG models. Each trend of the analytic functions was successfully predicted by the regression analysis, and the optimal subset of the basis function for the mean structure of the OTKG model was selected by the iterative optimization process. The selected basis functions were used to form an optimized mean structure for the OTKG model, significantly improving on the accuracy of the kriging model. The validation results verified that the proposed OTKG model provided a more accurate response surface than the existing OKG and UKG models. In this section, we will deal with a practical engineering problem to confirm the feasibility of the proposed framework and the OTKG model.

4.1 Problem definition

The practical engineering problem used for validation of the proposed model is a shape optimization of the two-dimensional RAE2822 airfoil, which is a transonic airfoil extensively used as a baseline model for design optimization. Studies have been conducted on various freestream flow conditions by P. H. Cook et al. [26]. In this study, the flow conditions included a Mach number of 0.725 and an angle of attack of 2.92 degrees. For these flow conditions, the transonic flow around the RAE2822 airfoil produces a strong shock on its upper surface that leads to dramatically increased drag. It is called wave drag, which also causes a considerable amount of total energy loss and results in decreased lift force. This wave drag can be reduced by changing the shape of the airfoil. Shape functions, such as PARSEC [27], NURBS [28], and the Hicks–Henne bump function [29], are needed to define or modify the geometric shape of the airfoil. In this study, Hicks–Henne bump functions have been used to modify the upper shape of the RAE2822 airfoil where the strong normal shock occurs. The detailed mathematical expression can be found in Eq. (22) where w_i is a weight factors that determine the changed shape. In the Fig. 8, the blue solid line indicates the upper and lower surfaces of RAE2822 airfoil and black dashed lines indicate the shapes of Hicks-Henne bump functions with respect to the chord location. Only three Hicks–Henne bump functions (f_2(x), f_3(x), and f_4(x)) are applied to change the shape of the upper airfoil surface. Therefore, the design variables for the shape optimization of the RAE2822 airfoil are the three weight factors of the Hicks–Henne bump functions (w_2, w_3, and w_4). Depending on the weight factor values, only the upper surface of the airfoil will be perturbed. The lower and upper bound of the design variables are -0.01 and 0.01, respectively. Meanwhile, the weight factors for other Hick–Henne bump functions (w_1 and w_5) remain unchanged at zero during the design optimization process, so that they cannot affect the modification of the airfoil shape.

$$y = y_o + \sum_{i=1}^{5} w_i f_i(x) \qquad f_i(x) = \begin{cases} \dfrac{\sqrt{x}(1-x)}{e^{15x}} & i = 1 \\ \sin^3\left(\pi x^{c_i}\right) & i = 2,3,4 \\ \dfrac{\sqrt{x}(1-x)}{e^{20x}} & i = 5 \end{cases} \quad \text{where} \quad C_i = \frac{\log(0.5)}{\log((i-1)/5)} \tag{22}$$

A detailed description of the practical application is included in Table 5. The number of initial sample points has been changed from 40 to 70 and randomly extracted by the LHS method. Regression analysis for 40 consecutive trials with different sets of the additional sample points is carried out to identify the trend of the true response. The results of the trend identification from the regression analysis show that the true response function has a strong

nonlinear trend along the w_2, w_3, and w_4 directions. Therefore, the 2nd order UKG model must be selected as the baseline model for constructing the OTKG model.

Table 5 Detailed description of practical application with three design variables

Parameter	Values
Number of design variable	3
Bound of design variable	$w_i \in [-0.01, 0.01]$, $i = 2, 3, 4$
Coefficient of determination for linear	0.3566
Coefficient of determination for nonlinear	(0.9575, 0.8438, 0.7756)

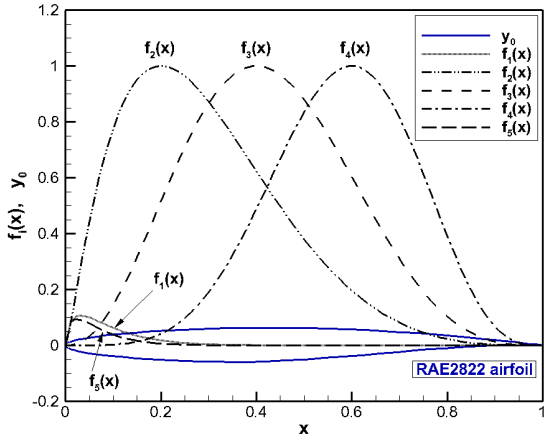

Fig. 8 Hicks–Henne bump functions and shape of RAE2822 airfoil.

4.2 Numerical function evaluation

Function evaluation for the set of sample points must be conducted to construct the kriging model. In this research, the KFLOW CFD solver was employed to investigate the flow characteristics around the RAE2822 airfoil and obtain the aerodynamic coefficients corresponding to modified shape of the airfoil. It has been developed and its accuracy and ability validated by previous studies [30, 31, 32]. This solver can provide reasonable flow solutions for both Euler and Reynolds Averaged Navier–Stokes (RANS) equations, and these governing equations are discretized using the cell-centered based Finite Volume method (FVM). For function evaluation of the candidate, we adopted the RANS equation to consider the viscous flow effect. The Roe's Flux-Difference Splitting (FDS) scheme [33] with a 3rd order Monotonic Upstream-Centered Scheme for Conservation Laws (MUSCL) [34] is used for the high order interpolation, and Harten's entropy correction function for avoiding non-physical phenomenon is used to resolve the

convective flux terms in the governing equation. In addition, the MUSCL scheme requires a limiter function. A limiter function can suppress the non-physical oscillation of solution in the flow region, containing strong discontinuities such as shock, by artificially reducing the interpolation slopes of the flow variables. Therefore, we adopted the minmod limiter function to prevent a spurious solution near the shock region. Menter's k-ω Shear Stress Transport (SST) turbulence model [35] is used to evaluate turbulence viscosity. Time integration is conducted with the Diagonalized-Alternating Direction Implicit (D-ADI) method [36] to obtain a converged steady solution.

The computational grid for the numerical simulation of the RAE2822 airfoil problem is a single-block and two-dimensional C-type topology with dimensions of 257×65. To accurately capture the boundary layer flow near the wall, the normal distance of the first grid near the airfoil surface is 0.0001c, where c is a chord length of the airfoil. The y+ value based on the size of the first grid is nearly close to unit. The no-slip and far-field boundary conditions are imposed on the boundaries of the wall and the far-field, respectively, to consider the viscous effect and prevent reflected disturbances back into the flow field. The computational grid system around the airfoil must be deformed in accordance with the changed shape of the airfoil. The grid deformation module is integrated into the CFD flow solver to handle the surface variation and automatically generate the new computational grid. The modified shape of the airfoil is determined by the summation of the original shape of the airfoil and the perturbed shape defined from the three Hicks–Henne bump functions, and the grid in the domain is smoothly deformed to adjust to the modified geometry with the trans-finite interpolation (TFI) method. Interpolating the neighboring grid points for dynamic mesh deformation in structured grids is a useful technique; it can preserve the grid quality of the initial grid [37].

Fig. 9 shows the surface pressure coefficient comparison between the predicted results from the numerical simulation and the experimental data. As can be observed in Table 6, the comparison results verify that the numerical simulation using the CFD solver can capture the flow phenomena around the RAE2822 airfoil, including the strong shock on the upper surface and provide significantly accurate function values at the sample points.

Table 6 Results of solver validation

	C_l	C_l error (present)	C_d	C_d error (counts)
Experiments (P.H. Cook et al.)	0.80300		0.01680	
CFD (present)	0.82358	2.56	0.01717	3.72

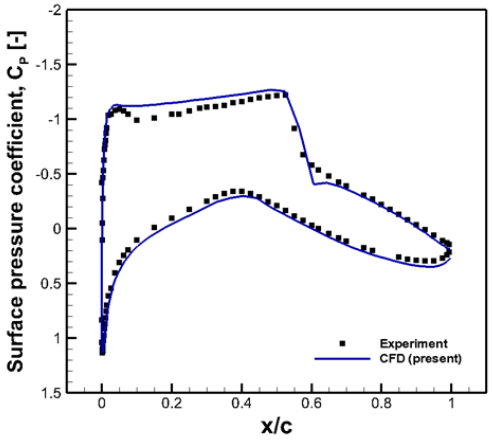

Fig. 9 Surface pressure coefficient comparison between experimental data and numerical results.

4.3 Results and discussion

The OKG, UKG, and proposed OTKG model were applied to the shape optimization problem for the RAE2822 to approximate the true response surface defined by three weight factors of the Hicks–Henne bump functions. Like the model comparison using the analytic function, the sums of the true RMSEs were compared. The exact function values at grid points were directly computed from CFD analysis. This model comparison was carried out over 40 trials with different sample profiles, given the number of the initial sample points. The number of initial sample points has also been changed from 40 to 60.

As listed in Table 7 and Fig. 10, as with the previous model comparison using the analytic functions, these results showed that the OTKG model resulted in the most accurate response compared to the OKG and other UKG models, regardless of the number of samples. It is notable that the OTKG model became the well-matured model despite the lack of sample points compared to the other models; other models required more sample points to achieve the level of accuracy of the OTKG model. The number of initial sample points can be insufficient to build an accurate kriging model. If the models are not mature enough to yield accurate prediction at untried points because of a lack of sample points, they must be refined by adding additional sample points. In general, if the additional sample points are added in the design space, the accuracy of the kriging models will gradually improve, and the error will be reduced. However, a lot of computing time might be required to conduct function evaluation for one sample point in a practical design problem. Even though the proposed OTKG model will require some time to find a set of optimal basis functions, it can efficiently yield a more accurate response surface compared to existing kriging

models. Fig. 11 illustrates shows the results from one trial for the practical problem with three design variables. It indicates the true error contours along the w_3 direction, depending on the kriging models. The true error contours show that the error of the OTKG model is the smallest at all positions.

Table 7 Mean true RMSEs over 40 trials of practical problem with three design variables

m	OKG	UKG1	UKG2	OTKG
40	0.1225	0.1079	0.1028	0.0848
50	0.1215	0.1067	0.0897	0.0787
60	0.1114	0.0955	0.0817	0.0722

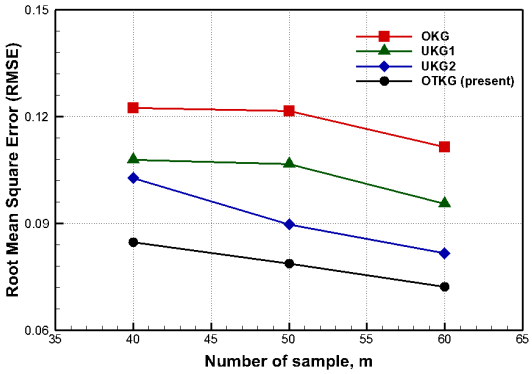

Fig. 10 Comparison of true RMSEs for practical problem.

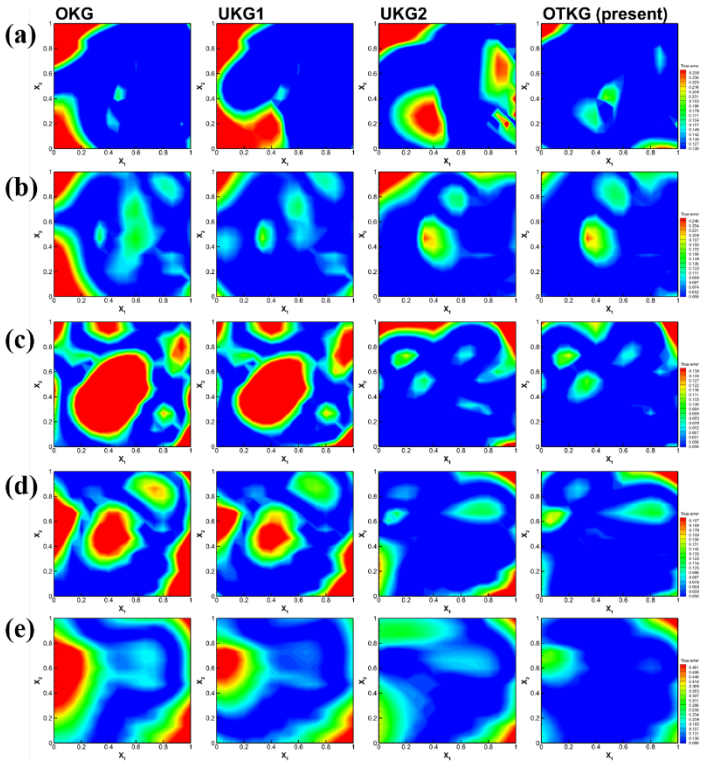

Fig. 11 Comparison of true error contours along w_3 direction for practical problem: w_3/D = (a) 1.0, (b) 0.75, (c) 0.50, (d) 0.25, and (e) 0.0

The model comparison was also conducted for a five-dimensional design problem. In order to calculate the effect of shape modification on the leading edge of airfoil, the weight factors of the Hicks–Henne bump functions $f_1(x)$ and $f_5(x)$ were included in the design variables. The total number of design variables was five, and the number of initial sample points was 70. The points were randomly extracted from the design domain using the LHS method. Regression analysis showed that the design variables w_2, w_3, and w_4 have a strong nonlinear trend. Meanwhile, the coefficients of determination for nonlinear design variables w_1 and w_5 were close to 0. Therefore, the 2nd order UKG model was chosen as the baseline model. The mean structure of the baseline model consists of a total of 21 basis functions. We found the set of optimal basis functions that could minimize error and increase the accuracy of the model in order to construct the OTKG model using the proposed framework. Unlike the model comparison of analytic functions and practical problem with three design variables, the sums of the model RMSEs which is objective function in the process of optimal basis function selection, were compared. As a result, its accuracy has been increased compared to other models by excluding unnecessary terms from the fixed form of the mean structure, as shown in Table 8.

Table 8 Mean model RMSEs over 40 trials of practical problem with five design variables

m	OKG	UKG1	UKG2	OTKG
70	0.1555	0.1525	0.1123	0.0935

5. Conclusion

In this research, the OTKG model was suggested to improve the accuracy of an existing TKG model. To construct the OTKG model, a framework including two key processes was introduced. One key process is trend identification, which is based on regression analysis, to approximately predict the true response. Regression analysis was carried out to assess the coefficients of determination and identify whether the true response has a linear or nonlinear trend. If the coefficients of determination for linear or nonlinear trends are greater than 0.5, the true response might have the corresponding trend. Thus, we can approximately predict the trend of the true response though the regression analysis and determine the most suitable order of the kriging model, (considering the trend of the true response). The second key process is the selection of the optimal basis functions using a global optimization algorithm. The fixed form of the mean structure in the UKG model globally represents the trend of the true response. However, it could lead to decreased accuracy of the model, since the fixed form of the mean structure might include unnecessary basis function terms. In the OTKG model, the optimal subset of the basis function, rather than the full set of basis function, is used to form the mean structures that could represent the true response more accurately. In this research, the optimization problem for selecting optimal basis functions from all of the candidates of basis function was solved using a binary-coded genetic algorithm. The minimization of an integrated mean square error was set as the objective function.

The proposed OTKG model was validated against two- and three-dimensional analytic functions and applied to solve a shape optimization problem for the RAE2822 airfoil. Model comparison using analytic functions verified that the proposed framework for constructing the OTKG can accurately predict the global trend of the true response and can successfully find the optimized subset of the basis function. The numerical results showed that the mean structure of OTKG model has been optimized to maximize the accuracy of kriging model depending on trend of true response, and it can significantly improve the accuracy of model by excluding unnecessary terms from full set of basis function. As a result, the proposed model provided the most accurate response surface with the lowest error

compared to existing kriging models. It is observed that the optimized trend kriging model can properly represent the true response despite the lack of initial sample points and can converge into a well-trained response surface with few additional sample points. It is worth noting that the proposed model could be more efficient and less computationally expensive way to construct accurate response surface for complex design problem, which require a high computational cost for iterative function evaluation, such as high-fidelity or unsteady CFD simulations.

However, the proposed OTKG model has some limitations. First, the coefficients of determination are merely statistical values evaluated from regression analysis. If they are slightly larger than 0.5, then the trend of the true function cannot be exactly identified. Second, the results of trend identification and the selection of the optimal basis function are significantly affected by the number of initial sample points, sample profiles, and the quality of the preliminary kriging models. In this research, the model comparisons for validation and application were carried out over 40 trials with different sets of the sample points to confirm the sampling dependency. The results showed that the OTKG model robustly represented the most accurate response surface compared to other models regardless of the number of sample points. Third, for the OTKG model, a supplementary calculation is required to perform regression analysis and find the optimal subset of the basis function. To prevent heavy computation for constructing OTKG model, the preliminary response surfaces are used to compute the function values for the regression analysis and the correlation parameter has remained constant during the selection process of optimal subset of basis function.

Appendix

The optimal subsets of the basis function selected by the proposed framework are listed in Table 9. They have been employed to construct the mean structure of the OTKG model. The total number of full basis functions can easily be computed by the formulation of ${}_{n+p}C_p$, where n is the number of design variables (the dimension of the design space) and P is the order of the baseline UKG model. During the process of optimal basis selection, only the polynomial terms that can accurately approximate the trend of the true response and minimize the error are chosen. For test function 1, only the nonlinear polynomial terms are selected to represent the true response along both the x_1 and x_2 directions, while the linear polynomial terms and correlated terms are totally excluded. The regression analysis results also show that the true response has a strong nonlinear trend along the x_1 and x_2 directions, and the coefficient of determination for the linear trend was very close to 0. These results from the regression analysis indicated that the basis functions have survived. Therefore, the proposed framework could improve on the quality of the kriging model by predicting the unknown trend

of the true response and accurately selecting the optimal subset of the basis function.

Table 9 Optimally selected subset of basis function

Case	Total number of full basis function	Optimally selected subset of basis function
Test function 1	6	$\mathbf{f}_{opt} = [1 \; x_1^2 \; x_2^2]$
Test function 2	10	$\mathbf{f}_{opt} = [1 \; x_1^2 \; x_1x_2 \; x_2^2 \; x_2x_3]$
RAE2822 with 3 design variables	10	$\mathbf{f}_{opt} = [1 \; x_2 \; x_3 \; x_1^2 \; x_1x_3 \; x_2^2 \; x_3^2]$
RAE2822 with 5 design variables	21	$\mathbf{f}_{opt} = [1 \; x_3 \; x_4 \; x_5 \; x_2^2 \; x_2x_4 \; x_3^2 \; x_3x_4 \; x_4^2]$

Acknowledgments

This research was supported by the Climate Change Research Hub of KAIST (Grant No. N11170061). This work was also supported by the Korea Institute of Energy Technology Evaluation and Planning(KETEP) and the Ministry of Trade, Industry & Energy(MOTIE) of the Republic of Korea (No. 20168520021200)

References

[1] Hao, P., Wang, B., and Li, G., "Surrogate-Based Optimum Design for Stiffened Shells with Adaptive Sampling," AIAA Journal, Vol. 50, No. 11, 2012, pp. 2389-2407.
doi: 10.2514/1.J051522

[2] Elanayar, S.V.T., and Shin, Y.C., "Radial basis function neural network for approximation and estimation of nonlinear stochastic dynamic systems," IEE Transactions on Neural Networks, Vol. 5, No. 4, 1994, pp. 594-603.
doi: 10.1109/72.298229

[3] Vijayaraghavan, V., Castagne, S., "Sustainable manufacturing models for mass finishing process," *The international Journal of Advanced Manufacturing Technology*, Vol. 86, 2016, pp. 49-57
doi: 10.1007/s00170-015-8146-3

[4] Vijayaraghavan, V., Garg, A., Gao, L., Vijayaraghavan, R., and Lu, G., "A finite element based data analytics approach for modeling turning process of Inconel 718 alloys," *Journal of Cleaner Production*, Vol. 137, 2016, pp. 1619-1627
doi: 10.1016/j.jclepro.2016.04.010

[5] Smola, A.J. and Schoelkopf, B., "A tutorial on support vector regression," *Statistics and Computing*, Vol. 14, 2004, pp. 199-222.
doi: 10.1023/B:STCO.0000035301.49549.88

[6] Powell, M.J.D., "Radial basis functions for multivariable interpolation: a review," *Algorithms for approximation*, Clarendon Press New York, NY, USA, 1997, pp.143-167.

[7] Krige, D.G., "A Statistical Approach to Some Basic Mine Valuation Problems on the Witwatersrand," *Journal of the Chemical, Metallurgical and Mining Engineering Society of South Africa*, Vol. 52, No. 6, 1951, pp. 119–139.
doi:10.2307/3006914

[8] Chung, H.S., and Alonso, J.J., "Using gradients to construct co-kriging approximation models for high-dimensional design optimization problems," *40th AIAA Aerospace Sciences Meeting and Exhibit*, Reno, Nevada, USA, 14-17 January, 2002, AIAA 2002-0317.

[9] Han, Z.-H., Zimmerman, R., and Görtz, S., "A new cokriging method for variable-fidelity surrogate modeling of aerodynamic data," *48th AIAA Aerospace Sciences Meeting Including the New Horizons Forum and Aerospace Exposition*, Orlando, Florida, USA, 4-7 January, 2010, AIAA 2010-1225.

[10] Han, Z.-H., Görtz, S., and Zimmermann, R., "Improving variable-fidelity surrogate modeling via gradient-enhanced kriging and a generalized hybrid bridge function," *Aerospace Science and Technology*, Vol. 25, No. 1, 2013, pp.177–189.
doi: 10.1016/j.ast.2012.01.006

[11] Joseph, V.R., Hung, Y., and Sudjianto, A., "Blind kriging: A New Method for Developing Metamodels," *Journal of Mechanical Design*, Vol. 130, No. 3, 2008, pp.031102.
doi:10.1115/1.2829873

[12] Zhao, L., Choi, K.K., and Lee, Ikjin, "Metamodeling Method Using Dynamic Kriging for Design Optimization," *AIAA Journal*, Vol. 49, No. 9, 2011, pp.2034–2046.
doi:10.2514/1.J051017

[13] Liang, H., and Zhu, M., "Comment on "Metamodeling method Using Dynamic Kriging for Design Optimization"," *AIAA Journal*, Vol. 51, No. 12, 2013, pp.2988–2989
doi: 10.2514/1.J052490

[14] Liang, H., Zhu, M., and Wu, Zhe., "Using Cross-Validation to Design Trend Function in Kriging Surrogate Modeling," *AIAA Journal*, Vol. 52, No. 10, 2014, pp.2313–2327
doi: 10.2514/1.J052879

[15] Kwon, H.I., and Choi, S.I., "A trended Kriging model with R indicator and application to design optimization," *Aerospace Science and Technology*, Vol. 43, 2015, pp.111–125.
doi:10.1016/j.ast.2015.02.021

[16] Matheron, G., *Le krigeage universel*, Les Cahiers du Centre de morphologie mathématique de Fontainebleau, Fascicule 1, École nationale supérieure des mines de Paris, France, 1969.

[17] Iman, R.L., Davenport, J.M., and Zeigler, D.K., "Latin Hypercube Sampling (a program user's guide)," Technical Report SAND 79-1473, Sandia National Laboratories, Albuquerque, New Mexico(NM), USA, 1980.

[18] Martin, J.D., and Simpson, T.W., "A Study on the Use of Kriging Models to Approximate Deterministic Computer Models," *ASME 2003 International Design Engineering Technical Conferences and Computers and Information in Engineering Conference*, Chicago, Illinois, USA, 2-6 September, 2003, DETC2003/DAC-48762, pp.567-576.

[19] Koehler, J.R., and Own, A.B., *Computer Experiments*. Handbook of Statistics, Elsevier Science, New York, Vol. 13, 1996, pp. 261–308.

[20] Abt, M., and Welch, W.J., "Fisher information and maximum-likelihood estimation of covariance parameters in Gaussian stochastic processes," *The Canadian Journal of Statistics*, Vol. 26, No. 1, 1998, pp.127–137.
doi: 10.2307/3315678

[21] Zimmerman, D., Pavlik, C., Ruggles, A., and Armstrong, M.P., "An experimental comparison of ordinary and universal Kriging and inverse distance weighting," *Mathematical Geosciences*, Vol. 31, No. 4, 1999, pp. 375–389.
doi: 10.1023/A:1007586507433

[22] Martin, J.D., and Simpson, T.W., "Use of Kriging Models to Approximate Deterministic Computer Models," *AIAA Journal*, Vol. 43, No. 4, 2005, pp.853–863.
doi: 10.2514/1.8650

[23] Deb, K., Pratap, A., Agarwal, S., and Meyarivan, T., "A fast and elitist multi-objective genetic algorithm: NSGA-II," *IEEE Transaction on Evolutionary Computation*, Vol. 6, No. 2, 2002, pp.182–197.
doi: 10.1109/4235.996017

[24] Kim, H.K., "Node-Based Spacecraft Radiator Design Optimization," Ph.D. Dissertation, Korea Advanced Institute of Science and Technology (KAIST), Daejeon, Republic of Korea, 2014.

[25] Wang, B., Hao, P., Li, G., Wang, X.J., Tang, X.H., and Luan, Y., "Generatrix shape optimization of stiffened shells for low imperfection sensitivity," *Science China Technological Sciences*, Vol. 57, No. 10, 2014, pp. 2012-2019.
doi: 10.1007/s11431-014-5654-6

[26] Cook, P.H., McDonald, M.A., and Firmin, M.C.P., "Aerofoil RAE 2822 - Pressure Distributions, and Boundary Layer and Wake Measurements," Experimental Data Base for Computer Program Assessment, AGARD Report AR 138, 1979.

[27] Sobieczky, H., "Parametric Airfoils and Wings," *Notes on Numerical Fluid Mechanics (NNFM)*, Vol. 68, 1998, pp.71–88.

[28] Piegl, L., and Tiller, W., *The NURBS Book,* 2nd ed., Springer-Verlag New York, Inc. New York, USA, 1997.

[29] Hicks, R.M., and Henne, P.A., "Wing Design by Numerical Optimization," *Journal of Aircraft*, Vol. 15, No.7, 1978, pp.407–412.
doi: 10.2514/3.58379

[30] Sa, J.H., Kim J.W., Park, S.H., Park, J.S., Jung, S.N., and Yu, Y.H., "KFLOW Results of Airloads on HART-II Rotor Blades with Prescribed Blade Deformation," *International Journal of Aeronautical and Space Sciences*, Vol. 10, Issue 2, 2009, pp.52–62.
doi: 10.5139/IJASS.2009.10.2.052

[31] Park, S.H., Lee, J.E., and Kwon, J.H., "A Preconditioned HLLE Method for Flows at All Mach Numbers," *AIAA Journal*, Vol. 44, No. 11, 2006, pp.2645–2653.
doi: 10.2514/1.12176

[32] Ko, J.H., Kim, J.W., Park, S.H., and Byun, D.Y., "Aerodynamic analysis of flapping foils using volume grid deformation code," *Journal of Mechanical Science and Technology*, Vol. 23, 2009, pp.1727–1735.
doi: 10.1007/s12206-009-0411-7

[33] Roe, P.L., "Approximate Riemann solvers, parameter vectors and difference schemes," *Journal of Computational Physics*. Volume 43, Issue 2, 1981, pp.357–372.
doi: 10.1016/0021-9991(81)90128-5

[34] Kurganov, A., and Levy, D., "A third-order semi-discrete central scheme for conservation laws and convection–diffusion equations," *Society for Industrial and Applied Mathematics (SIAM) Journal on Scientific Computing (SISC)*, Vol. 22, No. 4, 2000, pp.1461–1488.
doi:10.1137/S1064827599360236

[35] Menter, F.R., "Two-equation eddy-viscosity turbulence models for engineering applications," *AIAA Journal*, Vol. 32, No. 8, 1994, pp.1598–1605.
doi: 10.2514/3.12149

[36] Chang, M.J., Chow, L.C., and Chang, W.S., "Improved alternating-direction implicit method for solving transient three-dimensional heat diffusion problems," *Numerical Heat Transfer, Part B: Fundamentals: An International Journal of Computation and Methodology*, Vol. 19, Issue 1, 1991, pp.69–84.
doi: 10.1080/10407799108944957

[37] Dubuc, L., Cantariti, F., Woodgate, M., Gribben, B., Badcock, K.J., and Richard, B.E., "A grid deformation technique for unsteady flow computations," *International Journal for Numerical Methods in Fluid*, Vol. 32, Issue 3, 2000, pp. 285–311.
doi: 10.1002/(SICI)1097-0363(20000215)32:3<285::AID-FLD939>3.0.CO;2-C